Failure modes of coatings on steel substrate

K.P. MRÓZ[1]*, S. KUCHARSKI[1], K. DOLIŃSKI[1], A. BIGOS[2], G. MIKUŁOWSKI[1],
E. BELTOWSKA-LEHMAN[2], and P. NOLBRZAK[3]

[1] Institute of Fundamental Technological Research, Polish Academy of Sciences, 5B Pawińskiego St., 02-106 Warsaw, Poland
[2] Institute of Metallurgy and Materials Science Polish Academy of Sciences 25 Reymonta St., 30-059 Cracow, Poland
[3] Lodz University of Technology, 1/15 Stefanowskiego St., 90-924 Lodz, Poland

Abstract. The critical monotonic strain of Ni-W and $MoS_2(Ti,W)$ coatings on steel substrates was studied. The idea of axisymmetric bending test (called here as coin bending test) limited to monitoring of the coating failure was used. Experiments revealed mechanism of the coating failure, as cracking initiated from coating surface defects and/or substrate was demonstrated using indentation technique. By pushing the center of the uncoated side of a circular plate, the axisymmetric stress state was generated in the coating. The stress components varied gradually from the greatest value in the center to the smallest value at the edge of the specimen. The changes of the sample surface as a result of loading were monitored step by step via optical microscopy.

Key words: Ni-W coating, $MoS_2(Ti,W)$ coating, steel substrate, fracture, coatings strength, axisymmetric bending test.

1. Introduction

The objective of the deposition of the coating is the introduction of the different properties on the surface of the substrate material. Thin coatings are applied for decoration, increase corrosion resistance, wear resistance, electrical properties, solderability, etc. [1]. The thickness of coatings is from nanometers to several hundred micrometers. Their mechanical properties are crucial to preserve the usefulness of the products.

Generally, the degradation phenomena directly depend on the adhesion and cohesion strengths of the coating – substrate system. In the most cases the delamination (adhesive failure) at interface and coating cracking (cohesive failure) are the main modes of degradation of the structure. The poor adhesion means that the adhesive strength is not sufficient to withstand the stresses in the interface resulting from the external loading. Numerous studies have also been devoted to the failure of coated layers and correlation between the ability of cracks to traverse an interface undeflected and the bond strength of the interface [2,3]. A variety of recognized methods that are not always based on any physically explicit principles can be used to determine how well a coating is bonded to the substrate, e.g. knife test (ASTM D6677), tape test (ASTM D3359), scrape tests (ASTM D2197), pull-off tests (ASTM D4541, ISO 4624), scratch test (ASTM G171, ASTM C1624) and other. There are also some methods that enable us to determine the degree of adhesion (bonding strength) of a coating to a substrate or the cohesion strength of the coating, especially when the tension normal to interface is applied, e.g. ASTM C633. The indentation technique while the indenter load is continuously monitored as a function of the penetration depth during loading and unloading as well as the hardness tests in which the possible chip-off or other material behaviour can be identified are also used to characterise coatings. Nevertheless, the most useful and popular method

to characterise the coating-substrate system remains still the simple tension test. However, the standard mechanical tests need relatively large specimens, which are often not possible to obtain, especially for the coated specimens. Therefore, over the past three decades a number of testing techniques with miniaturised specimens has been developed. One of such techniques is the small punch (SP) testing proposed by Manahan et al. [4]. It appeared that the yield stress, strain hardening, and ultimate tensile strength estimated from the small punch test and those mechanical properties determined from the uniaxial tensile test show the reasonable correlations [5].

In the present work the idea of the small punch test was employed to monitor the coating failure as a result of the axisymmetric bending of a circle specimen. This experimental technique, called as the coin bending test, has been used to study the strength of two different coatings on the steel substrates: Ni-W and $MoS_2(Ti,W)$. The coatings were deposited on one side of the specimens. The changes of the surfaces on the coated side of a sample were monitored step by step under loading. The samples were examined by the use of optical microscopy and indentation techniques for assessing the development and degree of the coating damage.

2. Experimental details

2.1. Coatings.

Ni-W coatings. The electrochemical deposition (also called electrodeposition) is one of the most commonly used techniques for preparation of the adherent metallic coatings to improve the different properties of the bulk material [1]. Electrodeposition from aqueous electrolyte solutions (at a temperature lower than $100°C$), as a cheap and simple method, is a superior technique for manufacturing Ni-W coatings. It enables to obtain a uniform covering surface with simultaneous controlling of its thickness, microstructure and thus allows to

*e-mail: kmroz@ippt.pan.pl

K.P. Mróz, S. Kucharski, K. Doliński, A. Bigos, G. Mikułowski, E. Beltowska-Lehman, and P. Nolbrzak

design the properties of the coatings. Many researchers have synthesized nanocrystalline Ni-W alloys for evaluating a variety of its properties [6]– [12].

The Ni-W coatings were electrochemically deposited from sulfate-citrate electrolyte solution containing analytically grade purity chemicals: $NiSO_4 \cdot 7H_2O$, $Na_2WO_4 \cdot 2H_2O$ of a concentration ratio W(VI)/Ni(II) equal to 2 (0.2 M and 0.1 M, respectively). Sodium citrate ($Na_3C_6H_5O_7 \cdot 2H_2O$) at a concentration (0.3 M) equal to the sum of the concentrations of the electrodeposited metals was used as a complexing, buffering and leveling agent. The pH was adjusted to 8 by concentrated H_2SO_4 from the beginning value of 8.9. No brighteners, detergents and wetting agents were used. The electroplating of Ni-W coatings was carried out at 60°C, under the galvanostatic regime at 5 A/dm^2, in a system with a rotating disk electrode (RDE), under constant hydrodynamic conditions corresponding to the RDE rotation speed of 510 rpm. Low carbon steel disks (0.07 dm^2) DC powered by PAR273A potentiostat/galvanostat were used as a cathode. Prior to each experiment, the steel substrates were degreased, mechanically and chemically polished (in the solution of hydrogen peroxide and oxalic acid at 35°C) and then rinsed in distilled water in ultrasounds. As an anode a platinum wire (0.5 dm^2) was used. The obtained metallic, compact and well adherent to the steel substrate Ni-W (47.7% wt. W) coatings were characterised by a nanocrystalline microstructure, with the average grain size 10 nm [13, 14].

However, during the electrodeposition of the metallic coatings, hydrogen is evolved as a side reaction of the cathodic process. The hydrogen may diffuse into the steel lattice (substrate) causing delayed embrittlement when the component is subjected to a load. The hydrogen effect during the plating processes of Zn-Ni and Cd coatings has been investigated by Hillier and Robinson [15], but the amount of hydrogen generated by the coating process has not been well documented. Recently Mróz et al. [16] have studied the fatigue response of electrodeposited Ni-W on the low carbon steel substrate using the non-standard test specimens. They found that the coated specimens under stress control show lower fatigue resistance for higher stress amplitudes than their non-coated counterparts. However, for lower stress amplitude the fatigue strength of the both types of specimens was similar. Interestingly, that for the cyclic loading when the stress amplitude was bigger than a certain stress value the fatigue cracks started always at defects on the coating surface in the middle of each specimens. In contrast, for specimens loaded with lower stresses the fatigue damage started at the edge of the samples without any damage of the coating surface in the middle of the specimen. It might be explained as a result of the high yield stress of the Ni-W coatings compared with that of the steel substrate. It would make the surface defects less significant (active) than the effect of the substrate edge and/or its imperfections to initiate the fatigue crack formation for small values of loads.

MoS$_2$(Ti,W) coatings. The MoS$_2$ coatings were deposited by means of magnetron sputtering method in the reactive chamber of B.90 equipment described in details in paper [17]. During deposition process four magnetron sources were used. One of them was equipped with metallic Ti target, another one with metallic W target, and remaining two with sintered MoS$_2$ with addition of 12 at.% Ti. The sputtering of metallic Ti target was used to deposit technical interlayer of 50 nm thickness as described in details in [18]. The purpose of interlayer deposition was to improve the coating adhesion to metallic substrate. Metallic substrates used for MoS$_2$(Ti,W) coating were prepared with the same procedure. After being grinded and polished the substrates were cleaned with detergent and acetone in ultrasound cleaner. As some control samples the monocrystalline Si wafers were used. The deposition process was preceded with chamber pumping till the pressure of $9 \cdot 10^{-4}$ Pa was reached. After this value was achieved Ar flow was opened to the pressure of ∼3 Pa in the reactive chamber. Next the argon plasma glow discharge cleaning process of 720 ks was started. Afterwards the Ar flow was closed and reactive chamber was pumped till the pressure of $9 \cdot 10^{-4}$ Pa was reached again and then Ar flow was reopened to reach the pressure of $3.5 \cdot 10^{-1}$ Pa. When this value was achieved and stabilized the interlayer deposition process was started. Subsequently the final MoS$_2$(Ti,W) was deposited. During the whole deposition process the substrate bias was equal to −25 V. Microstructure and selected tribological properties of MoS$_2$(Ti,W) coatings were described in [19] paper.

Experiment. The non-standard type of specimens in form of disks of the radius $r = 15$ mm coated on one side were employed. The total thickness of the disks was ∼2 mm, of which ∼20 μm constituted the coating in the Ni-W case, or ∼2.2 μm in MoS$_2$(Ti,W), (Fig. 1). The steel disks of S235JRC cold-drawn and K340 (manufactured by Böhler) were prepared by Electrical Discharge Machining (EDM) BP-05d ZAPbp. The mechanical properties of S235JRC steel were verified from the uniaxial tensile tests, where yield stress, $\sigma_{YS} = 350$ MPa, ultimate tensile strength, $\sigma_{UTS} = 570$ MPa and maximum elongation, $\varepsilon_f = 16\%$ were reported. The chemical composition of the base material is given in Table 1 whereas the tension curve is presented in Fig. 2a.
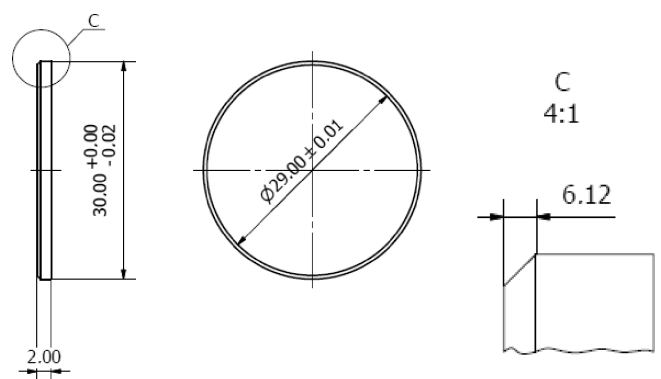

Fig. 1. Specimen geometry (dimensions in mm)

Table 1
Chemical composition of the S235JRC steel substrate

C	Mn	Si	P	S	Cu	N$_2$
0.13	0.31	0.18	0.009	0.023	0.01	0.005

Table 2
Chemical composition of the K340 steel substrate

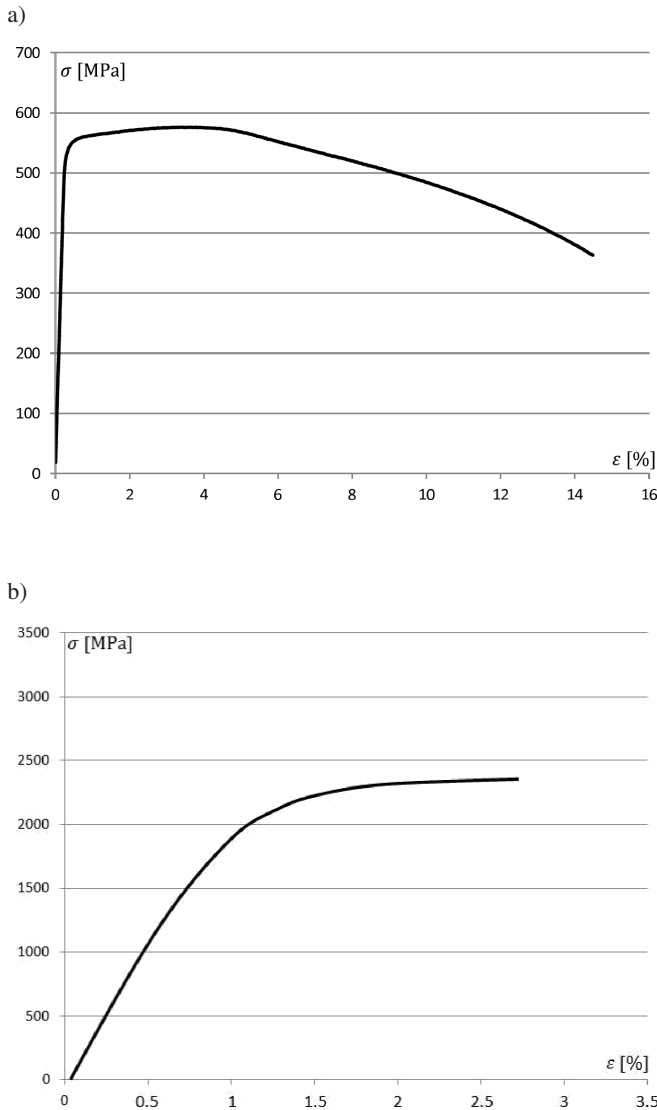| C	Si	Mn	Cr	Mo	V	additions
1.10	0.90	0.40	8.30	2.10	0.5	+

a)

b)

Fig. 2. Tension curve for the steel substrate: a) S235JRC, b) K340
(manufacturer Böhler)

The standard tensile tests were conducted in accordance with the ASTM standard E8M-04 using a servo-hydraulic material testing machine (MTS, Eden Prairie, MN US). The testing assembly consisted of: servo-hydraulic actuator MTS 244.12, axial force transducer MTS 661.19-F04, axial extensometer MTS 634.12F-25 (measurement base 25 mm). The properties of the mechanical K340 steel were determined from the uniaxial tensile tests and reported as follows: yield stress, $\sigma_{YS} = 2064$ MPa, ultimate tensile strength, $\sigma_{UTS} = 2350$ MPa and maximum elongation, $\varepsilon_f = 2.74\%$. The chemical composition of the steel is presented in Table 2 whereas the tension curve is presented in Fig. 2b.

In the paper the idea of the axisymmetric bending test limited to monitoring of the coating failure was used to study the strength of the coatings on the steel substrate. A special handle was designed and constructed to allow the testing of the atypical samples (Fig. 3) while the pressing element of the radius $r = 5$ mm was used.
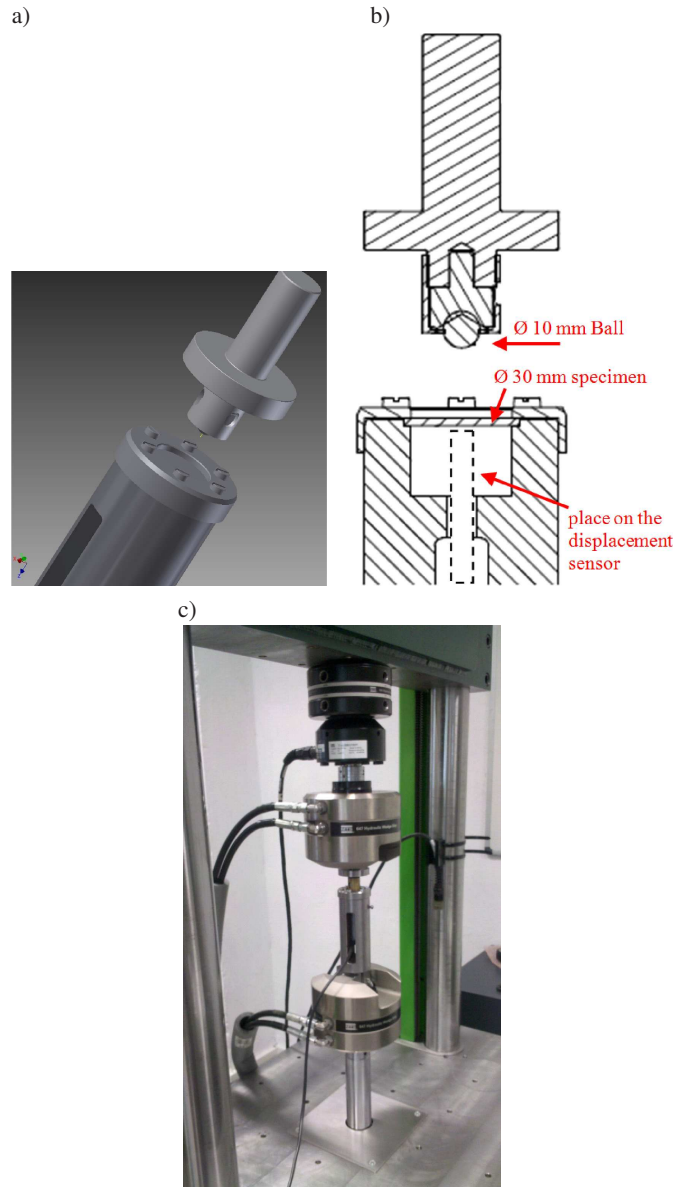
a)

b)

c)

Fig. 3. Handle designed and used in experiments

The coatings were deposited on one side of the specimens. The coated side was not loaded directly. Under pushing the center of the uncoated side, the axisymmetric stress state was generated in the coating and substrate. The stress components varied gradually from the greatest value in the center to the

smallest value at the edge of the specimen. It allowed us to observe the reaction of the coating to the different stress values at any intensity of the external loading. Simultaneously, after the critical loading when some damage appeared on the surface, it was possible to observe the evolution of the damage (usually in form of a crack) when the load increases. The changes of the sample surfaces under loading were monitored step by step. The samples were examined via optical microscopy and indentation techniques for assessing the development, degree and types of the coating damage. The coating strength was evaluated in terms of the applied loading required to initiate the fracture of the already existing defect on the surface. The loading applied to the sample increased step-by-step, Fig. 4.
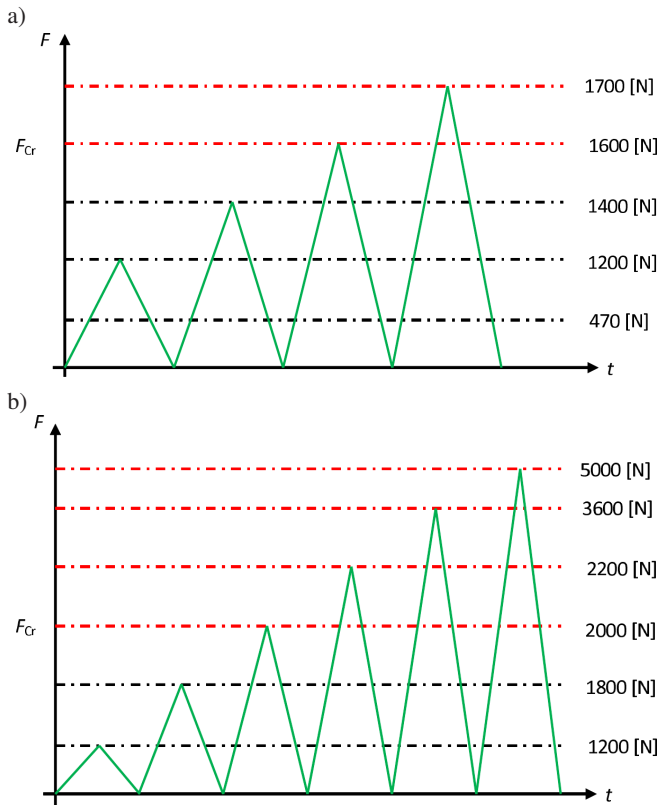

Fig. 4. Steps of loading for: a) Ni-W coating, b) MoS_2(Ti,W) coating

The tests were conducted at the room temperature. The displacement at the center of a sample was measured using LVDT (Linear Variable Differential Transducer) sensor. The resolution of the sensor was about 0.0002 mm. The deflection (displacement) and load were digitally recorded.

The changes of the sample surface resulting from the applied loads were monitored step by step with optical zoom. The CSM Open Platform equipment was used to perform Vickers hardness measurements in micro-scale. In the microindentation test, the displacement resolution and load resolution were 0.3 nm and 0.1 mN, respectively. To detect defects on the investigated thin layers, the scanning profilometer (Hommel-Etamic T8000 Nanoscan), with vertical resolution less than 1 nm, was used.

3. Results

3.1. Surface observations. Most frequently, despite the efforts of the manufacturers the coating contains defects such as pores. The pores (voids) are generally formed irrespectively of the preparation method as long as the deposition process involves a phase transformation [20]. The porosity reduces macroscopic ductility since the strains are concentrated in the vicinity of the pores and reduce the macroscopic flow stress. In the case of electrodeposited coatings, one of many factors affecting the porosity is small nonconducting areas on the substrate. It also seems to be possible for the steels used in the present investigation. Figure 5 shows an example of a sample with the transverse and hemispherical pores that extend almost through the investigated Ni-W coatings. The thickness of the layer can be estimated as about 20 μm. Whereas the topography and profile of one of the defects generated on the MoS_2(Ti,W) coating surface is presented in Fig. 6. The thickness of this layer can be estimated as about 2.2 μm.
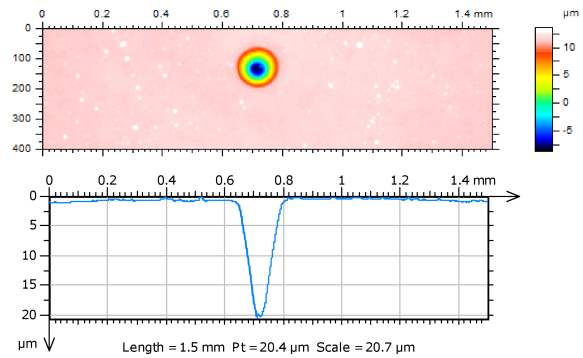

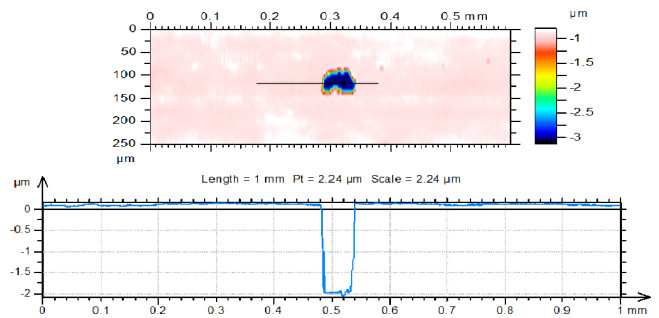Fig. 5. Hole with the measurement of the pore extends through Ni-W coating

Fig. 6. Defect with the measurement of extends through MoS_2(Ti,W) coating

3.2. Strength loading results. Generally, the degradation phenomena directly depend on the adhesion and coating strengths. In the most cases the delamination at interface and coating cracking are the main modes of degradation of the coating-substrate system. In Ni-W coating case the delamination at interface was not observed. In contrast the coating cracking beginning at the circular defects in the centre of the specimen was reported, Fig. 7. The critical fracture loading for investigated coating was estimated as 1400-1600 N, Fig. 4. Similarly, degradation of the MoS_2(Ti,W) coating begins on

irregular pore in the centre of the specimen, Fig. 8a under critical loading estimated as 1800–2000 N, Fig. 8b.
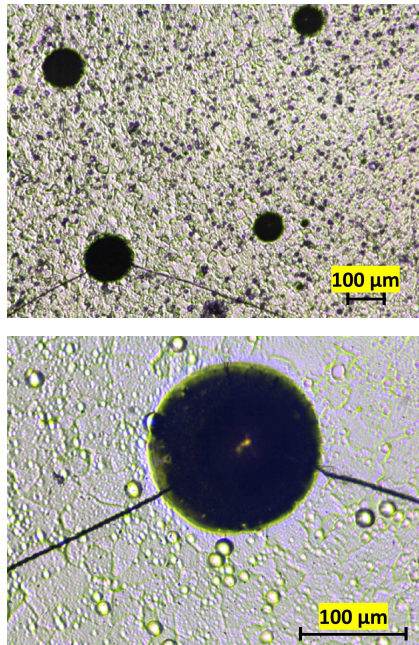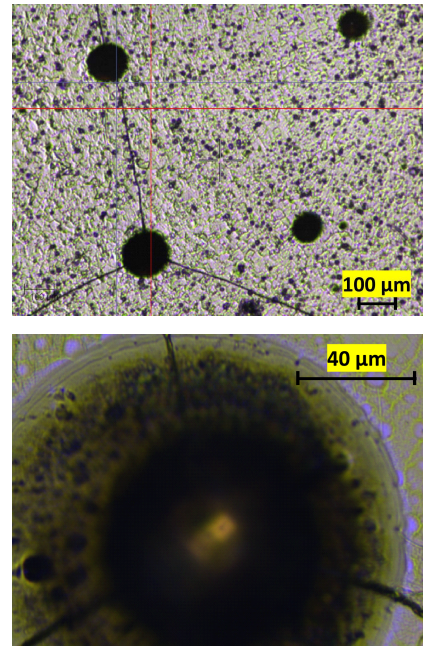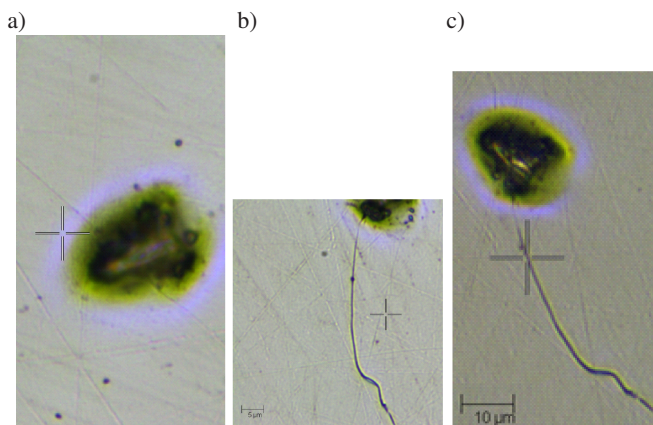

Fig. 7. Ni-W coating after 1600 N

Fig. 8. MoS$_2$(Ti,W) coating under: a) $F = 0$ N, b) under $F = 2000$ N, c) under $F = 3600$ N and $F = 5000$ N without any change of the crack length

We assume, that in an initial stage of damage, due to very small thickness of the coating, the strain in coating is practically the same as the strain at the surface of substrate. Then, knowing the substrate mechanical characteristics, Fig. 2 and using FEM tools (for example Abaqus 6.10 software) the critical substrate strain is obtained (assuming non-influence of the coating) as $\varepsilon_{Cr} \approx 0.84\%$ and $\varepsilon_{Cr} \approx 0.34\%$ for Ni-W and MoS2(Ti,W), respectively. Since the relatively good homogeneity of the pore distribution on the surface was observed for Ni-W coatings the randomness of the size and location of defects had no effect on the critical loading level. Moreover, with an increase of load it was possible to observe the propagation of the cracks, Fig. 9, connecting the pores and forming a crack net, eventually, Fig. 10.
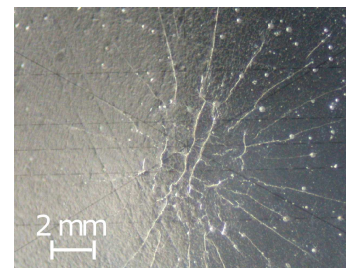

Fig. 9. Ni-W coating after 1700 N

Fig. 10. Ni-W coating after 4000 N

In contrast, the behaviour of MoS$_2$(Ti,W) coating for loading $F > 2000$ N inducing the strain bigger than the critical strain $\varepsilon_{Cr} \approx 0.34\%$ was not so clear. There was no increase of length of the crack initiated at the pore, as depicted in Fig. 8b-c, but quite different crack patterns were observed on the surface layer, Fig. 11. Hence to clarify the problem, in a vicinity of the cracks the nanoindentation tests with Berkovich tip and micro-indentation tests with spherical tip ($R = 20$ μm) were performed. In some cases, for larger loads, the destruction (fracture) of a certain fragment of the layer around the residual imprint took place. Once the layer debris have been removed, the surface of substrate in the damaged region was visible. These small areas (scars) with removed layer, Fig. 12b enable us to analyze the substrate surface more in detail. The specific scratch patterns are visible on the substrate surface and it can be noticed that some of these shallow scratches have the same directions as the scratches observed on the surface of coating. The photography and AFM image of the surface of substrate inside the scar are presented in Fig. 13. Thus, it can be concluded that the topography of the substrate is reproduced on the layer surface. It is a result of a specific technology of layer deposition. The residual impressions generated in microindentation tests are visible on layer and slightly less distinct – on the substrate. In Figs. 12b, 13a, one

can observe two residual imprints after the indentation tests – both were performed with the same load in the apparently undamaged layer. However, the first one did not devastate the layer. In contrast, in the vicinity of the second one the layer was completely damaged and some debris of the layer remain visible. One can conclude that in the location of the second imprint the layer has been already detached from the substrate surface i.e. prior to the indentation the local delamination process took place caused by the bending test.

It can be seen that the scratch patterns on the substrate surface are similar as the patterns of coating cracks generated in the bending test, cf. Figs. 11b and 12b. Therefore, the substrate scratches can be one of the reason of initiation of damage (cracking and/or delamination) of the layer.
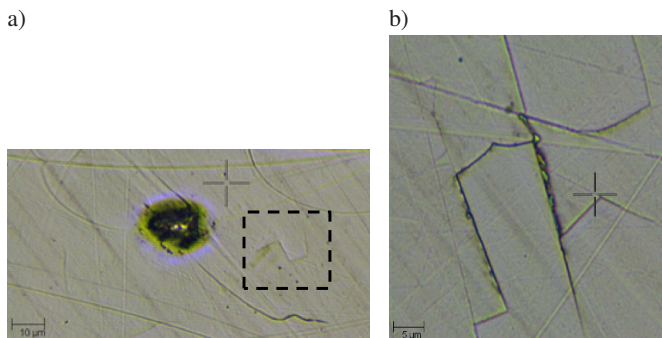
a)

b)

Fig. 11. Evolved characteristic defect on the MoS$_2$(Ti,W) coating after $F = 5000$ N with specific observed surface failure
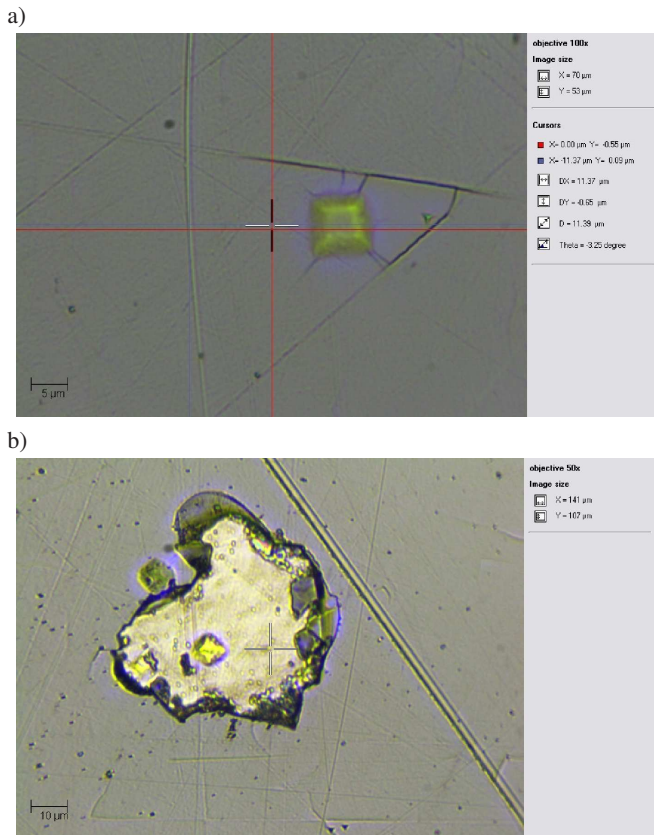
a)

b)

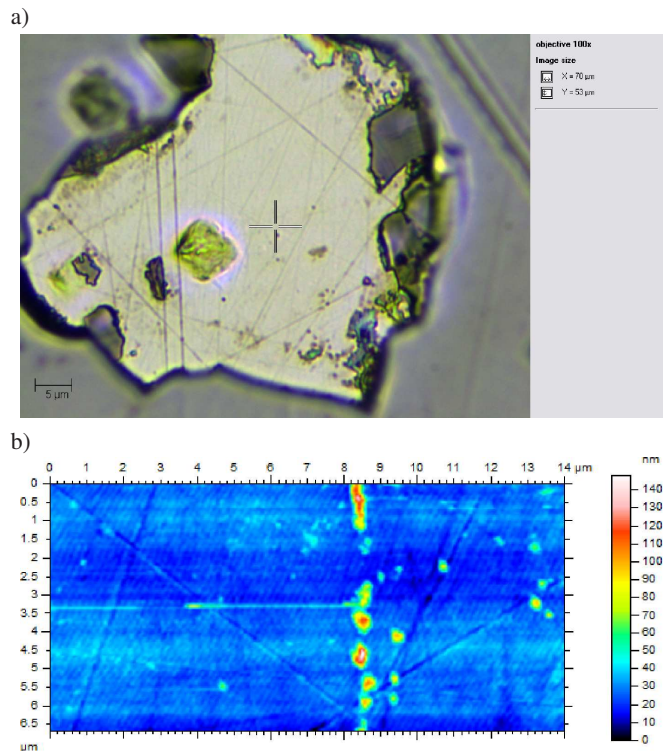Fig. 12. Chipping MoS$_2$(Ti,W) coating step by step after $F = 5000$ N

a)

b)

Fig. 13. Surface of substrate with scratches and residual imprint of MoS$_2$(Ti,W) coating after 5000 N

3.3. Mechanical properties of coatings specified in nanoindentation tests.
The indentation test is a convenient and sometimes a unique method for determining the material properties of thin coatings. One of important quantities measured in indentation test is hardness H, usually interpreted as a mean contact pressure. There were many attempts to estimate constitutive properties of the material on the basis of hardness measurements, however the problem is still open and there is no generally accepted method to obtain the values of yield and tensile strengths using hardness measurements. The fundamental experimental investigations of hardness were performed by Tabor [21] and Johnson [22]. The numerical simulation of indentation tests with sharp indenters was presented in a series of papers by Giannakopoulos and Larsson [23]–[25]. The exhaustive report concerning a correlation between the hardness and tensile strength for steels has been presented in [26].

There is a simple formulae that correlates the hardness with the yield stress for unstressed damaged specimens proposed in [26], i.e.

$$\sigma_y = -90.7 + 2.876\,H_V, \qquad (1)$$

where the yield stress is in MPa and H_V is a diamond pyramid hardness in [kgf/mm^2]. To specify hardness and Young modulus (Oliver-Pharr method) of the coatings, the nanoindentation tests with Berkovich tip were performed prior to the bending test. The penetration depth has not exceeded 1/10 of the coating thickness. In the case of the MoS$_2$ coating it was less than 150 nm. Hardness and Young modulus of the

$MoS_2(Ti,W)$ and Ni-W layers specified in nonoindention test are HIT = 7600 MPa, E = 95 GPa and HIT = 7800 MPa, E = 195 GPa, respectively. It means that the yield stress can be estimated as about 2200 MPa and 2400 MPa for $MoS_2(Ti,W)$ and Ni-W, respectively.

The similar yield stress values of the investigated coatings with a very large difference in Young modules indicate a higher critical strain value for $MoS_2(Ti,W)$ coating than for Ni-W layers. However, the values measured on the basis of the proposed coin bending test are completely opposite. One of the reason for that might be an effect of the different forms (shapes) of the characteristic stress concentrators observed on the coating surface, see Figs. 9 and 14. As a result the effective (actual) critical strain calculated using FEM for specimens with $MoS_2(Ti,W)$ is lower than that calculated for specimens with Ni-W coating. For fair comparison the local strain generated in both kinds of defects should be calculated. Another explanation is that the yield stress estimated from indentation test corresponds to a compressive stress, while in the bending test we induce the tensile stress. It should be also noted that the Eq. (1) was calibrated for metals, where high value of hardness is associated with much higher value of Young modulus than that estimated for the investigated $MoS_2(Ti,W)$ coating. Therefore, the used equation may not be actually valid for $MoS_2(Ti,W)$ coating because the constitutive law that describes plastic behaviour of this coating is not known. However the loading-unloading penetration depth curves measured in nanoindentation test for this coating appear to be qualitatively similar to that observed in the case of nanoindentation of metals. Thus, the elastic-plastic behaviour of the coating is assumed to be similar to the behaviour of metals. Hence, a certain amount of plastic strain would be admissible in the coating without crack initiation and consequently the Eq. (1) is fulfilled, at least approximately, for the coating.

Fig. 14. The depth and shape of the propagated cavity on $MoS_2(Ti,W)$ coating

In Ni-W coating the damage was initiated in small defects on the coating surface. In MoS_2 coating some cracks were initiated in defects, however for bigger loading specific crack patterns occurred also in the region where the surface defects were not observed. The cracks are probably initiated by the scratches on substrate surface generated prior to the

coating deposition during the sample preparation process. The microindentation test showed that some of the cracked areas were associated with delamination of the layer. Such behavior indicates on a mixed mode of damage of MoS_2 coating. We have observed that the location of delamination regions cannot be strictly correlated with local stress level resulting from the bending of a sample. It indicates that the the adhesion of the coating is not homogeneous on whole surface of sample.

4. Conclusions

The idea of the axisymmetric bending test limited to monitoring of the coating failure was used to study the strength of the coatings on the steel substrates. Coated specimens with Ni-W and $MoS_2(Ti,W)$, were investigated and the coating fracture due to the critical monotonic strain was demonstrated. The experiments revealed the mechanism of the initial coating failure, as cracking initiated from surface defects. The proposed investigation of the coating enabled us to observe the development of the damage under increasing loading. By pushing the center of the uncoated side, the axisymmetric stress state was generated in the coating. The stress components varied gradually from the greatest value in the center to the smallest value at the edge of the specimen. It allowed us to observe the reaction of the coating to different stress values at any intensity of the external loading. The changes of the sample surface under loading were monitored step by step via optical microscopy.

Bending, microindenation and nanoindetation tests enable us to investigate mechanical properties of coatings for different material scales to observe different modes of coating damage. The micro- and nanoindentation tests can be used to specify local mechanical properties of the layer (Young moduls, hardness) and to detect the regions where the delamination of the layer takes place due to previous bending test. In the proposed experimental procedure the different damage modes could be observed. One of them is cracking observed in the bending test initiated by the stress concentration at the surface defects in both coatings. For the specimens with $MoS_2(Ti,W)$ coating the substrate scratches are some origins of the stress concentration resulting in the layer cracking and, moreover, the delamination within the cracked regions is observed as a result of the prior bending.

Experiments confirmed that the critical strain, which can be specified from local measurements (for example from indentation technique), might exhibit bigger values than those obtained from macroscopic techniques. It should be taken into consideration when such coated elements are to be used in applications in which measured critical substrate strain is in question.

It should be also noted that the critical strain obtained in the presented experiments is valid for a specific coating-substrate system, only. In fact, the presence of the residual stresses, distribution and shape of defects as well as the substrate preparation prior coatings deposition all influence on results. To have more general characteristic of the coating one should perform experiments with a selected coating, e.g.
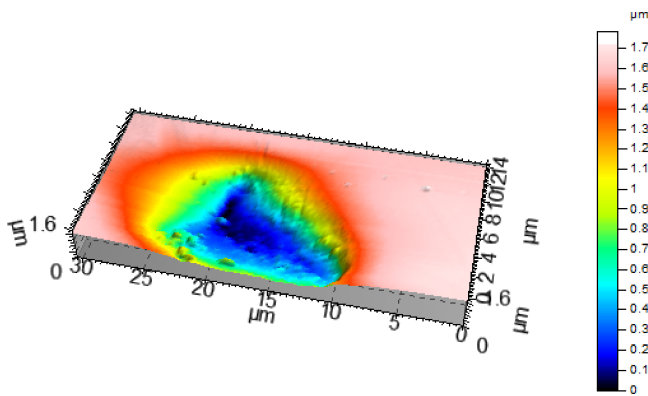
K.P. Mróz, S. Kucharski, K. Doliński, A. Bigos, G. Mikułowski, E. Beltowska-Lehman, and P. Nolbrzak

MoS$_2$(Ti,W) deposed on different substrates. It will be a subject of authors future investigations.

REFERENCES

[1] W.H. Safranek, *The Properties of Electrodeposited Metals and Alloys*, Elsevier, New York, 1974.

[2] K.P. Mróz and K. Doliński, "The crack growth prediction in homogeneous materials and bimaterial systems", *ZAMM – Zeitschrift für Angewandte Mathematik und Mechanik* 90, 721–744 (2010).

[3] Z. Mróz and K.P. Mróz, "Analysis of delamination and damage growth in joined bi-layer systems", *Geomechanics for Energy and the Environment* 4, 4–28 (2015).

[4] M. Manahan, A. Argon, and C. Harling, "The development of a miniaturised disk bend test for the determination of postirradiation mechanical properties", *J. Nucl. Mater.* 103–104, 1545–1550 (1981).

[5] G.E. Lucas, "Review of small specimen test techniques for irradiation testing", *Metallurgical Trans.* A 21A, 1105–1119 (1990).

[6] T. Yamasaki, P. Schlossmacher, K. Ehrlich, and Y. Ogino, "Formation of amorphous electrodeposited Ni-W alloys and their nanocrystallization", *Nanostructured Materials* 10, 375–388 (1998).

[7] T. Nasu, M. Sakurai, T. Kamiyama, T. Usuki, C. Uemura, and T. Yamasaki, *J. Non-Crystalline Solids* 319, 312–314 (2002).

[8] C.A. Schuh, T.G. Nieh, and H. Iwasaki, "The effect of solid solution W additions on the mechanical properties of nanocrystalline Ni", *Acta Materialia* 51, 431–443 (2003).

[9] D.B. Lee, J.H. Ko, and S.C. Kwon, "High temperature oxidation of Ni-W coatings electroplated on steel", *Material Science and Engineering. A, Structural Materials: Properties, Microstructure and Processing* 380, 73–78 (2004).

[10] H. Iwasaki, K. Higashi, and T.G. Nieh, "Tensile deformation and microstructure of a nanocrystalline Ni-W alloy produced by electrodeposition", *Scripta Materialia* 50, 395–399 (2004).

[11] H. Somekawa, T.G. Nieh, and K. Higashi, "Instrumented indentation properties of electrodeposited Ni-W Alloys with different microstructures", *Scripta Materialia* 50, 1361–1365 (2004).

[12] M. Ma, V.S. Donepudi, G. Sandi, Y.K. Sun, and J. Prakash, "Electrodeposition of nano-structured nickel-21% tungsten alloy and evaluation of oxygen reduction reaction in a 1% sodium hydroxide solution", *Electrochimica Acta* 49, 4411–4416 (2004).

[13] P. Indyka, E. Beltowska-Lehman, M. Faryna, and K. Berent, "Microstructural and microchemical characterization of the nickel-based thin films prepared by electrodeposition", *Archives of Metallurgy and Materials* 55, 421–427 (2010).

[14] P. Indyka, E. Beltowska-Lehman, L. Tarkowski, A. Bigos, and E. García-Lecina, "Structure characterization of nanocrystalline Ni-W alloys obtained by electrodeposition", *J. Alloys and Compounds* 590, 75–79 (2014).

[15] E.M.K. Hillier and M.J. Robinson, "Permeation measurements to study hydrogen uptake by steel electroplated with zinc-cobalt alloys", *Corrosion Science* 48, 1019–1035 (2006).

[16] K.P. Mróz, A. Bigos, S. Kucharski, K. Dolinski, and E. Bełtowska-Lehman, "Ni-W electrodeposited coating on the low carbon steel substrate – the fatigue observation", *J. Materials Engineering and Performance* 23, 3459–3466 (2014).

[17] B.G. Wendler, M. Danielewski, K. Przybylski, A. Rylski, L. Kaczmarek, and M. Jachowicz, "New type AlMo, AlTi- or Si-based magnetron sputtered protective coatings on metallic substrates", *J. Materials Processing Technology* 175, 427–432 (2006).

[18] T. Moskalewicz, S. Zimowski, B. Wendler, Nolbrzak P, and A. Czyrska-Filemonowicz, "Microstructure and tribological properties of low-friction composite MoS$_2$(Ti,W) coating on the oxygen hardened Ti-6Al-4V alloy", *Metals and Materials Int.* 20, 269–276 (2014).

[19] B. Wendler, T. Moskalewicz, M. Kot, S. Zimowski, A. Czyrska-Filemonowicz, W. Pawlak, A. Rylski, K. Wlodarczyk-Kowalska, P. Nolbrzak, and M. Makowska, "Modern self-lubricating coatings for automotive, aviation and spacecraft industry", *Materials Science Forum* 782, 31–38 (2014).

[20] J.W. Dini, *Electrodeposition. The Materials Science of Coatings and Substrates*, Noyes Publications, Westwood, 1993.

[21] D. Tabor, *Hardness of Metals*, Oxford University Press, Oxford, 1951.

[22] K.L. Johnson, "The correlation of indentation experiments", *J. Mechanics and Physics of Solids* 18, 115–126 (1970).

[23] A.E. Giannakopoulos, P.-L. Larsson, and R. Vestergaard, "Analysis of vickers indentation", *Int. J. Solids and Structures* 31, 2679–2708 (1994).

[24] P.-L. Larsson, E. Soderlund, A.E. Giannakopoulos, D.J. Rowclife, and R. Vestergaard, "Analysis of Berkovich Indentation", *Int. J. Solids and Structures* 33, 221–248 (1996).

[25] P.L. Larsson, "Investigation of sharp contact at rigid plastic conditions", *Int. J. Mech. Sci.* 43, 895–920 (2001).

[26] E.J. Pavlina and C.J. Van Tyne, "Correlation of yield strength and tensile strength with hardness for steels", *J. Materials Engineering and Performance* 17, 888–893 (2008).